Magnetic surface and magnetoelastic interface anisotropies in epitaxial Au/Co and Ag/Co superlattices

Toshiki Kingetsu* and Katsura Sakai†
Advanced Materials Research Laboratories, Nisshin Steel Company Ltd., 7-1 Koya-shinmachi, Ichikawa 272, Japan
(Received 11 February 1993)

In situ observations of reflection high-energy electron diffraction and Co-layer-thickness dependence of magnetic anisotropy in epitaxial (111)Au/Co, Ag/Co, Au/Co/Ag, and Ag/Co/Au superlattices indicate that the two interfaces of each Co layer in the Au/Co superlattices are not identical and that the magnetoelastic interface anisotropy arises only from the Au/Co interfaces formed upon depositing Co on Au layers. It has been demonstrated that the magnetoelastic interface and the Néel-type magnetic surface anisotropies contributing to the perpendicular magnetic anisotropy can be separately estimated. Saturation of magnetic anisotropy energy at small Co-layer thickness was discussed in terms of the gradient in Co-layer strains.

In recent years, there has been great interest in magnetic properties of metallic multilayers and superlattices from both the fundamental and application viewpoints. One such property is the perpendicular magnetic anisotropy and it has been attracting much attention in relation to magnetic and magneto-optical recording media.[1] As has been reported in several systems, such as Pd/Co (Ref. 2) and Pt/Co,[3] a large positive uniaxial magnetic anisotropy (K_{eff}) is observed in cases where the magnetic-layer thicknesses are thinner than several monolayers. As for the Au/Co and the Ag/Co superlattices, it has been reported that the Au/Co superlattices exhibit marked perpendicular anisotropy,[4–6] while the Ag/Co superlattices do not, at least at room temperature.[6–8]

In phenomenological approaches, the major possible origins of the perpendicular anisotropy are presently controversial and have been proposed to be the Néel-type magnetic-surface anisotropy (or magnetocrystalline surface anisotropy), which arises from reduced symmetry of the structure at interfaces, and magnetoelastic-interface anisotropy.[7,9–11] If the main origin is the magnetoelastic anisotropy, critical-thickness models based on the elastic and the dislocation formation energies[6,10] predict that the Ag/Co superlattices also have perpendicular anisotropy with a similar magnitude, since Au and Ag have nearly the same lattice constants and very similar mechanical properties. If the Néel-type surface anisotropy is the main origin in both the superlattices, Au/Co/Ag and Ag/Co/Au superlattices should have an average value of K_{eff}'s in the Au/Co and the Ag/Co superlattices with the same Co layer thicknesses. In the case of the magnetoelastic anisotropy, the situation should be also the same if both interfaces to Au of each Co layer make the same contribution to the perpendicular anisotropy.

In this paper we will show that the nature of the Co-layer interfaces depends on the sequence of deposition and that the magnetoelastic interface anisotropy originates only from the Au/Co interfaces formed upon depositing Co on Au layer in the Au/Co superlattices. We will also demonstrate that the perpendicular magnetic anisotropy consists of contributions from both the magnetoelastic interface and the Néel-type surface anisotropies, and that these two anisotropy contributions can be separately estimated.

The (111)Au/Co, Ag/Co, Au/Co/Ag, and Ag/Co/Au superlattices were grown at a substrate temperature of 373 K by molecular-beam epitaxy (MBE) using a VG Semicon V80M MBE system. Here, Au/Co/Ag denotes that Au is deposited first, and then Co and Ag are deposited sequentially. The superlattices are synthesized by repeating the trilayers or bilayers 20 times. As the substrate, (111)Si wafers were used and they were cleaned by heating at 1473 K for a short period to obtain 7×7-reconstructed surfaces. Then, growth of (111)Ag buffer layers on the substrates followed by annealing at 673 K for 1.2 ks was performed. Prior to superlattice growth, base layers of 10-nm thicknesses were grown on the buffer layers. The base layers were of Au for the Au/Co and the Au/Co/Ag superlattices and were of Ag for the Ag/Co and the Ag/Co/Au superlattices. Capping layers of Au or Ag were also grown, depending on the final species of the superlattices. The surface cleanliness was checked by Auger electron spectroscopy and x-ray photoelectron spectroscopy *in situ*. Structural characterization of the superlattices were made through *in situ* reflection high-energy electron diffraction (RHEED) during growth and x-ray diffraction (XRD) in air. Magnetization curves were obtained by a superconducting quantum interference device magnetometer at 300 K. Magnetic fields up to ±55 kOe were applied with directions both parallel and perpendicular to the film plane. The parallel fields were applied in $\langle 1\bar{1}0\rangle_{\text{Si}}$ and $\langle 2\bar{1}\,\bar{1}\rangle_{\text{Si}}$ directions.

The formation of the periodic structures was confirmed through XRD (θ–2θ scans) profiles both in the low- and the middle-angle regions. The orders of superlattice reflections observed were higher in the Au/Co and the Au/Co/Ag superlattices than in the Ag/Co and Ag/Co/Au superlattices. In the Au/Co and the Au/Co/Ag superlattices, reflections up to the seventh order were observed both in the low- and the middle-angle

regions.

RHEED patterns of the film surfaces indicated that the superlattices grew epitaxially and that interfaces between layers were parallel to the close-packed plane. The RHEED patterns of Co layers deposited on Ag layers were somewhat spotty and showed that the crystal structure of Co was hexagonal close-packed (hcp) after growth of several monolayers in thickness. This result agrees with our previous results.[8,12] The patterns were streaky in other cases and hence it was difficult to identify the crystal structure of Co on Au layers. However, in early reports,[4] the crystal structure of Co in MBE-grown (111)Au/Co superlattices has been shown to be hcp. The crystal structure of Co in our Au/Co and Au/Co/Ag superlattices is expected to be hcp. The epitaxial relations were, hence, found to be Si(111)$\langle 1\bar{1}0\rangle$/buffer Ag(111)$\langle 1\bar{1}0\rangle$/Au, Ag(111)$\langle 1\bar{1}0\rangle$/Co(0001)$\langle 11\bar{2}0\rangle$/Ag, and Au(111)$\langle 1\bar{1}0\rangle$.

The spacing of streaks in RHEED patterns is inversely proportional to an in-plane lattice constant of a deposited film surface. The relative in-plane lattice constant can thereby be estimated, and is shown in Fig. 1 as a function of layer thickness. Here, Figs. 1(a) and 1(b) are for an Au/Co/Ag and an Ag/Co/Au superlattice, respectively. It is found that in the Au/Co/Ag superlattices, Co layers grew pseudomorphically on the Au underlayers at the beginning and that their lattice constants decreased gradually toward their own magnitude in bulk with increasing Co layer thickness. On the other hand, in the Ag/Co/Au superlattices, Co layers grew on Ag underlayers with their own lattice constants in bulk and the Ag/Co interfaces were completely incoherent. These growth modes are similar to those in the Au/Co and the Ag/Co superlattices, respectively, which will be reported in a separate paper.[8] It is emphasized that Au layers on the Co underlayers grew incoherently in the Ag/Co/Au superlattices, as was the case with Ag on Co in the Ag/Co superlattices,[8,12] and contrary to the pseudomorphic growth of Au on Co layers at the beginning in the Au/Co superlattices.[8] This result means that Au layers can grow pseudomorphically only on the dilated Co layers, which were caused by depositing Co on the Au underlayers. Therefore, Co-Au atomic bonding is not strong enough to strain the Au layers deposited on the unstrained Co underlayers, for this type of Au/Co interfaces. This suggests that the Au overlayers do not strain the Co underlayers appreciably even in the case of Au/Co superlattices. From the above discussion, it is deduced that only the near-interface regions of the Co layers formed upon depositing Co on the Au underlayers are strained in the Au/Co superlattices.

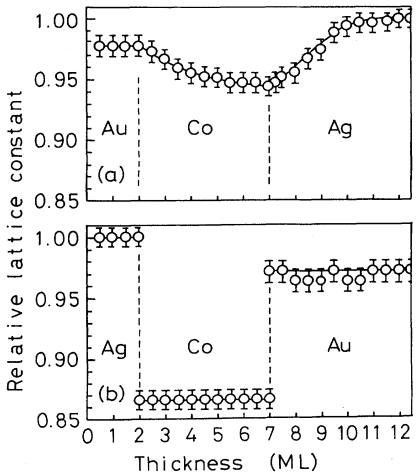

FIG. 1. Relative in-plane lattice constant as a function of layer thickness obtained from RHEED observations. The first trilayer in (a) Au/Co/Ag and (b) Ag/Co/Au superlattices.

Figure 2 shows magnetization curves of Au/Co and Au/Co/Ag superlattices with a Co layer thickness of about six monolayers, measured with applied fields both parallel and perpendicular to the film plane. It is clear that the easy axis of magnetization lies on the normal of the film plane for both the superlattices. The curves for the perpendicular fields are nearly the same in the two superlattices, while the curve for the parallel fields in the Au/Co/Ag superlattice reaches the saturation magnetization faster than that in the Au/Co superlattice, indicating that the perpendicular magnetic anisotropy in the Au/Co/Ag superlattice is weaker. It was found that there was no appreciable difference between the magnetization curves for applied fields parallel to the $\langle 1\bar{1}0\rangle_{Si}$ and the $\langle 2\bar{1}\,\bar{1}\rangle_{Si}$ directions on the film plane. The effective anisotropy K_{eff} was determined from the area between perpendicular and parallel magnetization curves per unit Co volume. The K_{eff} is positive when the magnetization is preferably oriented perpendicular to the film plane.

Figure 3 shows $K_{eff}t$ values of the four types of superlattices as a function of t, where t is the thickness of Co layers. It is clearly seen that the $K_{eff}t$-t relations for the Au/Co/Ag and the Ag/Co/Ag superlattices are distinctly different, despite the fact that each Co layer in both types of superlattices has an interface to Au and another interface to Ag. Especially, as was also shown in Fig. 2, the Au/Co/Ag superlattices exhibit perpendicular anisotropy when Co layers are several monolayers in thickness and tend to saturate for the smaller thickness, as is the case with the Au/Co superlattices. On the contrary, the shape of the plot for the Ag/Co/Au superlattices is linear and these superlattices show in-plane magnetic anisotropy, as is the case with the Ag/Co superlattices, although

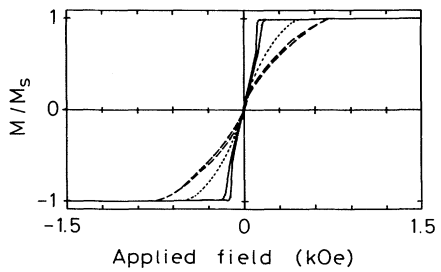

FIG. 2. Normalized magnetization (M/M_s) curves for Au/Co and Au/Co/Ag superlattices with a Co layer thickness of six monolayers. The solid curve is for both systems with field perpendicular to the film plane. The dashed and dotted curves are for Au/Co and Au/Co/Ag with parallel field, respectively.

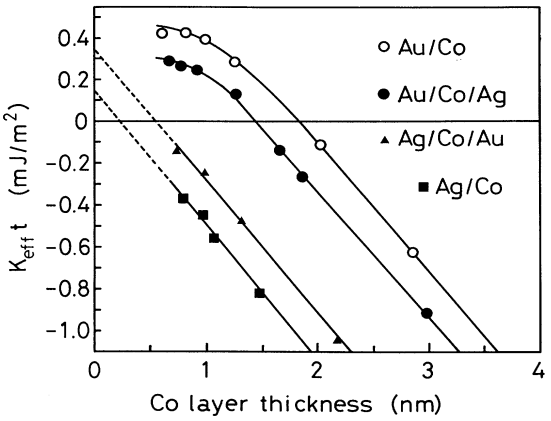

FIG. 3. Dependence of $K_{eff}t$ on t for Au/Co, Au/Co/Ag, Ag/Co/Au, and Ag/Co superlattices.

the $K_{eff}t$ values for the Ag/Co/Au superlattices are somewhat larger. The $K_{eff}t$ values for the Au/Co superlattices are substantially in good agreement with the published data for Au/Co superlattices,[4–6] and the linear dependence of $K_{eff}t$ on t in the Ag/Co superlattices also agrees with the results in previous work.[6,8] The difference between the $K_{eff}t$-t relation for the Au/Co/Ag and that for the Ag/Co/Au superlattices arises from the sequence of deposition, i.e., only the Co interface regions upon depositing Co on the Au layers are strained and contribute to the magnetoelastic interface anisotropy as shown below.

In a phenomenological approach, $K_{eff}t$ is often expressed as $K_{eff}t=2K_s+K_vt$, where K_s is the interface anisotropy, K_v is the volume anisotropy, and the factor of 2 arises from the two interfaces of each Co layer. If K_s and K_v are constants, this equation leads to a linear plot with an intercept of $2K_s$ at $t=0$. In the case of the present four types of superlattices, the inclinations of the linear portions of the four plots are nearly the same[13] ($K_v=-0.63$ MJ/m^3) and hence, the equation is rewritten as

$$K_{eff}t=(K_{s(Au)}^{(N)}+K_{s(Au)}^{(e)})+(K_{s(Au)}^{(N)}+K_{s(Au)}^{\prime(e)})+K_vt\ , \quad (1)$$

$$K_{eff}t=(K_{s(Au)}^{(N)}+K_{s(Au)}^{(e)}+K_{s(Ag)}^{(N)}+K_vt\ , \quad (2)$$

$$K_{eff}t=K_{s(Ag)}^{(N)}+K_{s(Au)}^{(N)}+K_vt\ , \quad (3)$$

$$K_{eff}t=2K_{s(Ag)}^{(N)}+K_vt\ , \quad (4)$$

for Au/Co, Au/Co/Ag, Ag/Co/Au, and Ag/Co, respectively. Here the superscripts (N) and (e) denote the Néel-type surface anisotropy and the magnetoelastic interface anisotropy, respectively, and subscripts (Au) and (Ag) correspond to Co interfaces to Au and Ag, respectively. $K_{s(Au)}^{\prime(e)}$ denotes the magnetoelastic interface anisotropy arising from the Au/Co interfaces formed upon depositing Au on the Co underlayers. It is noted that the magnetoelastic anisotropy in the linear regions are not included in K_v but included in K_s, although in the coherence-incoherence critical-thickness models[6] the coherency strains are included in K_v. From Eqs. (1)–(4), the values of $K_{s(Au)}^{(e)}$, $K_{s(Au)}^{(N)}$, and $K_{s(Ag)}^{(N)}$ are estimated to be 0.57, 0.27, and 0.07 mJ/m^2, respectively. $K_{s(Au)}^{\prime(e)}$ is approximately zero and this originates from the fact that the spacings of the linear plots between Eqs. (1) and (2) and between Eqs. (3) and (4) are nearly the same. This result is consistent with the RHEED results that only the Co interface regions upon depositing Co on the Au layers are strained, causing the magnetoelastic interface anisotropy. From the above discussion, it is concluded that the perpendicular magnetic anisotropy in the Au/Co superlattices consists of contributions from both the magnetoelastic interface and the Néel-type surface anisotropies. The apparent K_s value is $(K_{s(Au)}^{(e)}+2K_{s(Au)}^{(N)})/2=0.56$ mJ/m^2 and agrees with the 0.58 mJ/m^2 reported previously.[6]

From the RHEED results, strain distributions in the Co layers of the Au/Co and Ag/Co superlattices is expected and its simplified model is schematically shown in Fig. 4(a). Figure 4(b) is a high-resolution transmission electron micrograph (HRTEM) for a cross section of an Ag/Co superlattice grown on a 50-nm Ag buffer layer using a (0001) sapphire substrate in our previous work.[12] In this micrograph, edge-dislocation arrays in Co layers are clearly seen, showing the incoherency of the Ag/Co in-

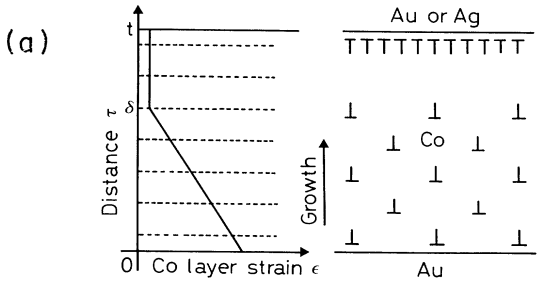

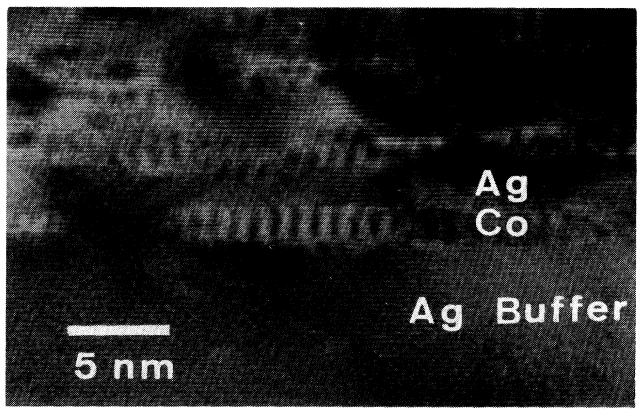

FIG. 4. (a) Scheme of the strain distribution and the possible location of misfit dislocations for Au/Co and Au/Co/Ag superlattices. A linear decay of strain was assumed. (b) Cross-sectional HRTEM micrograph of an Ag/Co superlattice grown on a 50-nm Ag buffer layer/(0001) sapphire substrate. Moiré fringes caused by misfit dislocation networks bounding in-plane microdomains are seen in Co layers. The spacing of the fringes is about 1 nm, which is half of the domain size expected from the lattice-constant difference, indicating hexagonal networks of edge dislocations.

terfaces, which is consistent with the RHEED results. HRTEM experiments for the Au/Co and the Au/Co/Ag superlattices are in progress and the results will be shown in future publication.

Next, we will discuss the nonlinear portions of the $K_{\text{eff}}t$-t plots. In early reports,[6] the deviation from the linear plot at small t in the Au/Co superlattices was attributed to sample growth problems such as island formation due to bad wetting. However, no appreciable deviation in the plot of the Co/Ag superlattices for similar t values indicates that this invocation is not appropriate, because similar or more severe problems are expected in the Ag/Co superlattices. We will show that these are more intrinsic properties in the Au/Co system. In the nonlinear portions, $K_{s(\text{Au})}^{(e)}$ is not a constant, and is expressed as

$$K_{s(\text{Au})}^{(e)} = \int_0^t K_{\text{ME}}(\tau)d\tau \ , \tag{5}$$

where $K_{\text{ME}}(\tau)$ is the magnetoelastic anisotropy of Co at the distance τ measured from the Au/Co interface formed upon depositing Co on Au. $K_{\text{ME}}(\tau)$ may be expressed as $K_{\text{ME}}(\tau)=-C\lambda\varepsilon(\tau)$, where λ is the magnetostriction constant, $\varepsilon(\tau)$ the strain[14] at position τ, and C the positive constant relating to the elastic-constant tensor. For simplicity, we assume that $\varepsilon(\tau)$ decays linearly to become a constant at $\tau=\delta$, as shown in Fig. 4(a). If Co-layer thickness t is larger than δ, the right-hand side of Eq. (5) becomes $(\varepsilon_1-\varepsilon_2)\delta/2+\varepsilon_2 t$, where ε_1 and ε_2 are strains at $\tau=0$ and $\tau=\delta$, respectively. Here, the term $\varepsilon_2 t$ should be included in the term $K_v t$ in Eqs. (1) and (2), rather than in K_s. This leads Eqs. (1) and (2) to linear plots. On the other hand, if t is smaller than δ, the right-hand side of Eq. (5) becomes $(\varepsilon_2-\varepsilon_1)t^2/2\delta+\varepsilon_1 t$, leading Eqs. (1) and (2) to parabolic plots with apex upper side. This discussion accounts for the saturation or a falloff of the $K_{\text{eff}}t$-t plots at small t.

In conclusion, we have shown that the nature of the Co layer interfaces depends on the sequence of deposition and that the magnetoelastic interface anisotropy originates only from the Au/Co interfaces formed upon depositing Co on Au layers in the Au/Co superlattices. The perpendicular magnetic anisotropy is found to consist of contributions from both the magnetoelastic interface and the Néel-type surface anisotropies. It has been demonstrated that these two anisotropy contributions can be estimated separately. The saturation of the $K_{\text{eff}}t$ value at small t is ascribed to the strain gradient in the Co layers. The Ag/Co superlattices do not exhibit perpendicular anisotropy. This is ascribed to the absence of the magnetoelastic anisotropy and the weakness of the Néel-type anisotropy ($K_{s(\text{Ag})}^{(N)}=0.07$ mJ/m^2).

The failure of the critical-thickness models proposed earlier[6,10] in interpreting the $K_{\text{eff}}t$-t relations is attributed to the implicit assumptions of uniform strains in Co layers and identities of two interfaces of each Co layer, and no consideration of the dissimilarity in interactions between Co atoms and nonmagnetic atoms such as Au and Ag atoms.

---

*Present address: Japan Ultra-high Temperature Materials Research Center, 573-3 Okiube, Ube, Yamaguchi 755, Japan.

†Present address: Forming Technology Development Laboratories, Nisshin Steel Company Ltd., Amagasaki 660, Japan.

[1] *Materials for Magneto-Optic Data Storage,* edited by T. Suzuki, C. Falco, and C. Robinson, MRS Symposia Proceedings No. 150 (Materials Research Society, Pittsburgh, 1989).

[2] P. F. Carcia, A. D. Meinhalt, and A. Suna, Appl. Phys. Lett. **47**, 178 (1985); B. N. Engel, C. D. England, R. A. Van Leeuwen, M. H. Wiedman, and C. M. Falco, Phys. Rev. Lett. **67**, 1910 (1991).

[3] Z. B. Zeper, F. J. A. M. Greidanus, P. F. Carcia, and C. R. Fincher, J. Appl. Phys. **65**, 4971 (1989); C.H. Lee, R. F. C. Farrow, C. J. Lin, E. E. Marinero, and C. J. Chien, Phys. Rev. B **42**, 11 384 (1990).

[4] C. H. Lee, Hui He, F. Lamelas, W. Vavra, C. Uher, and R. Clarke, Phys. Rev. Lett. **62**, 653 (1989).

[5] S. Araki, T. Takahata, and T. Shinjo, IEEE Trans. J. Magn. Jpn. **5**, 568 (1990).

[6] F. J. A. den Broeder, W. Hoving, and P. J. H. Bloemen, J. Magn. Magn. Mater. **93**, 5462 (1991).

[7] T. Kingetsu, K. Sakai, T. Kaneko, A. Yamaguchi, and R. Yamamoto, in *Thin Film Structures and Phase Stability,* edited by B. M. Clemens and W. L. Johnson, MRS Symposia Proceedings No. 187 (Materials Research Society, Pittsburgh, 1990), p. 309.

[8] T. Kingetsu and K. Sakai, J. Appl. Phys. **73**, 7622 (1993).

[9] P. Bruno, J. Phys. F **18**, 1291 (1988).

[10] C. Chappert and P. Bruno, J. Phys. (Paris) **64**, 5736 (1988); P. Bruno and J. -P. Renard, Appl. Phys. A **49**, 499 (1989).

[11] C. H. Lee, Hui He, F. J. Lamelas, W. Vavra, C. Uher, and R. Clarke, Phys. Rev. B **42**, 1066 (1990); R. Clarke, S. Elagoz, W. Vavra, and C. Uher, J. Appl. Phys. **70**, 5775 (1991).

[12] K. Sakai and T. Kingetsu, J. Cryst. Growth **126**, 184 (1993).

[13] In all four types of present superlattices, the crystal structure of Co is hcp. Hence, the nearly equal values of K_v are reasonable, since K_v is mainly related to the magnetocrystalline anisotropy and the demagnetization energy.

[14] Since the films would have some relaxation upon subsequent layer growth of superlattices, the direct use of the $\varepsilon(\tau)$ value obtained from the RHEED results may not be appropriate for the exact determination of the $K_{\text{ME}}(\tau)$ value. However, the strain gradient is expected to be retained to a certain extent.

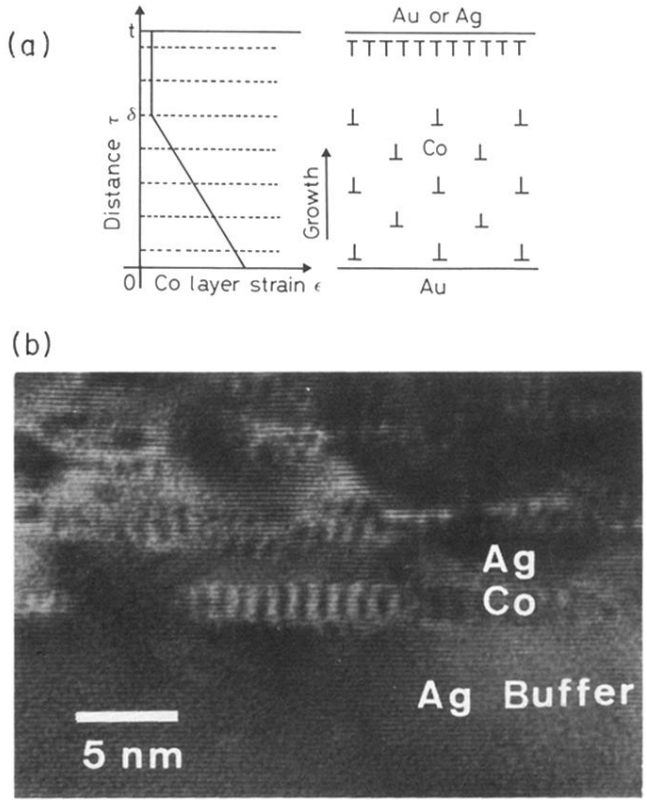

FIG. 4. (a) Scheme of the strain distribution and the possible location of misfit dislocations for Au/Co and Au/Co/Ag superlattices. A linear decay of strain was assumed. (b) Cross-sectional HRTEM micrograph of an Ag/Co superlattice grown on a 50-nm Ag buffer layer/(0001) sapphire substrate. Moiré fringes caused by misfit dislocation networks bounding in-plane microdomains are seen in Co layers. The spacing of the fringes is about 1 nm, which is half of the domain size expected from the lattice-constant difference, indicating hexagonal networks of edge dislocations.